

Microscopic state equation for oscillator chains

*Original*

Microscopic state equation for oscillator chains / DI FLORIO, Vincenzo; Giberti, Claudio; Rondoni, Lamberto; Zhao, Hong. - In: THE EUROPEAN PHYSICAL JOURNAL PLUS. - ISSN 2190-5444. - 139:7(2024), pp. 1-15.  
[10.1140/epjp/s13360-024-05419-1]

*Availability:*

This version is available at: 11583/2992561 since: 2024-09-17T16:32:52Z

*Publisher:*

Springer

*Published*

DOI:10.1140/epjp/s13360-024-05419-1

*Terms of use:*

This article is made available under terms and conditions as specified in the corresponding bibliographic description in the repository

*Publisher copyright*

(Article begins on next page)



## Microscopic state equation for oscillator chains

Vincenzo Di Florio<sup>1,2,4,a</sup> , Claudio Giberti<sup>3</sup>, Lamberto Rondoni<sup>1,4</sup>, Hong Zhao<sup>5</sup>

<sup>1</sup> Department of Mathematical Sciences, Politecnico di Torino, 10129 Turin, Italy

<sup>2</sup> Istituto Italiano di Tecnologia (IIT), Via Melen 83, B Block, Genoa, Italy

<sup>3</sup> Department of Sciences and Methods for Engineering, University of Modena and Reggio E., Via G. Amendola 2, Pad., Morselli, 42122 Reggio Emilia, Italy

<sup>4</sup> INFN, Sezione di Torino, Via P. Giuria 1, 10125 Turin, Italy

<sup>5</sup> Department of Physics, Xiamen University, Xiamen 361005, China

Received: 20 March 2024 / Accepted: 2 July 2024

© The Author(s) 2024

**Abstract** Systems allowing anomalous transport of mass, momentum energy, etc., such as low-dimensional particles systems or highly confining media, are hard to characterize thermodynamically. Indeed, local thermodynamic equilibrium may not be established and their behaviour often strongly depends on many microscopic parameters, including the symmetry of the interaction potentials. Thermodynamic state equations, on the other hand, involve a small set of observables, which are obtained averaging in time and over the large number of particles that populate mesoscopic cells in which local equilibrium can be realized. In this work we show that a linear relation discovered earlier, that connects the average distance between pairs of consecutive particles with their kinetic energy, applies to quite a large set of 1-dimensional particle systems known to produce anomalous transport. This relation is microscopic in nature, since the quantities involved are neither averaged over many particles, neither over very large times. Nevertheless, its robustness is under variations of the external parameters, and the limited set of quantities it involves qualify it as a state equation, analogously to thermodynamic relations. We provide conditions for which the relation can be violated within a limited range of parameters values, and we find that it can be extended to two-dimensional networks of coupled oscillators. The validity of this relation further shows that the states of aggregation of matter in low-dimensional systems are often different from standard macroscopic ones.

### 1 Introduction

The properties of 1-dimensional systems made of linearly or nonlinearly interacting oscillators are the subject of a vast literature, that began with the FPUT model [1], and then ramified in countless directions. Initially, the problem of energy equipartition, relaxation to equilibrium, and related ergodic notions were investigated. Later, energy transport in nonequilibrium conditions became most popular. See *e.g.* [2] for a selection of works concerning both phenomena. Chains of oscillators have been considered because of their simplicity and, more recently, because they appeared to enjoy some properties of nanotechnological interest [3]. While energy equipartition is fairly well understood [4–7], the transport of energy still poses numerous questions. One widely accepted view is that energy transport in FPUT-like 1-dimensional systems is typically anomalous, *i.e.* it violates Fourier law, although different and even contrasting points of view are found in the specialized literature, see *e.g.* [8–12]. One characteristic feature of anomalous transport is that bulk properties depend on the boundary conditions and, in particular, depend on the length of the chain. Therefore, local thermodynamic equilibrium<sup>1</sup> is not established [14–17]. Indeed, by its very definition, locality requires spatial correlations to decay within mesoscopic distances. Then, properties of matter in the bulk, such as the transport coefficients, are not affected by boundaries located “sufficiently far”, *i.e.* beyond a moderate number of mean free paths from the place of interest. For a detailed discussion of the local thermodynamic equilibrium condition see *e.g.* references [18] Chapter II Section 9, [19] Chapters 3–5, [20] Section 15.1, [21] Section 2.3, [22] Section 3.3, [23] Chapter 1, [24, 25]. It is clear that observables of small and low-dimensional systems are less likely to obey local thermodynamic equilibrium than 3-dimensional macroscopic systems, because spatial constraints hinder the decay of correlations. This constitutes part of the reasons leading to anomalous transport.

Interestingly, mean free paths are known to be unbounded in many 1-dimensional systems, so locality is violated, but in certain cases one may identify structures that interact over short distances and enjoy locality (high-frequency modes), while others do not, and lead to anomalous transport (low-frequency modes) [26]. This allows a consistent description of the phenomenon at hand. Furthermore, there are models and conditions under which transport turns normal even in 1-dimensional systems, see *e.g.* [2, 3,

<sup>a</sup> e-mail: [vincenzo.diflorio@polito.it](mailto:vincenzo.diflorio@polito.it) (corresponding author)

<sup>1</sup> Thermodynamic equilibrium is the fundamental property justifying the local mass, momentum and energy balances as thermodynamic relations [13].

27–29]. In particular, the symmetries of the oscillators interaction potentials have been found to play a important role in certain models [8–12]. This result can also be obtained by adding a strain to the chains [30].

Given the complexity of such a scenario, it is desirable to find relations describing the state of 1-dimensional systems in terms of a reduced number of variables, *i.e.* of counterparts of the thermodynamic equations of state, holding beyond standard thermodynamics. In this respect, it is interesting to recall the beginning of Section 9 of Ref. [18], which explains that different kinds of thermodynamic quantities exist “*Thermodynamic physical quantities are those which describe macroscopic states of bodies. They include some which have both a thermodynamic and a purely mechanical significance, such as energy and volume. There are also, however, quantities of another kind, which appear as a result of purely statistical laws and have no meaning when applied to non-macroscopic systems, for example entropy*”.

The relation discovered in Ref. [15] (Eq. (5) of that paper) and investigated in a handful of papers: [16, 17, 31, 32] seems to be a good candidate for such an equation of state. Indeed, we are going to show that it holds in a vast variety of cases, in which the boundary between purely mechanical and purely statistical quantities is blurred, both in absence and in presence of external drivings. Although it is reminiscent of the virial theorem of Clausius [33], we conclude that this relation does not derive straight from pure mechanics: it carries statistical information as well. At the same time, it is a microscopic kind of relation because it does not involve averaging over many particles or over very large times.

The rest of the article is organised as follows. In Sect. 2 we present and discuss the microscopic state equation and review the 1-dimensional particle systems on which it is tested. In Sect. 3, we numerically evaluate the validity of Eq. (7) for different potentials. In Sect. 4, we focus our attention on the behaviour of  $\beta$ -FPUT chains, giving an attempt at a theoretical explanation of our results. In this section the chain with stochastic baths is also considered. In Sect. 5, we validate the linear relation (7) for 2-dimensional nets. Finally, in Sect. 6, we draw our conclusions.

## 2 Models and the microscopic relation

In the present paper, we consider systems of  $N$  interacting oscillators of unit mass and positions  $x_i \in \mathbb{R}$ , with  $i = 1, \dots, N$ . In positions  $x_0$  and  $x_{N+1}$  we place particles that do not move and interact, respectively, with particle 1 and  $N$  like all oscillators do. In some cases, these walls repel the approaching moving particles, confining the dynamics within the interval  $[x_0, x_{N+1}]$ ; in other cases, they allow the moving particles to pass beyond them. Particles 1 and  $N$  also interact with deterministic or stochastic thermostats, of temperatures  $T_L$  and  $T_R$ , respectively. Letting  $r$  denote the difference of coordinates of particles with consecutive labels, *e.g.* ( $x_{i+1} - x_i$ ), the potential energies of the particles interactions we investigate are expressed by:

- Harmonic:  $V(r) = \frac{k}{2}(r - a)^2$  (1)

- Harmonic+hard core:  $V(r) = \begin{cases} \frac{k}{2} r^2 & \text{if } r > a \\ +\infty & \text{if } r \leq a \end{cases}$  (2)

- Soft-point:  $V(r) = \frac{1}{2} \left( r^2 + \frac{1}{r^2} \right)$  (3)

- Lennard-Jones:  $V(r) = 4\epsilon \left[ \left( \frac{\sigma}{r} \right)^{12} - \left( \frac{\sigma}{r} \right)^6 \right]$  (4)

- $\beta$ -FPUT:  $V(r) = \frac{g_2}{2}(r - a)^2 + \frac{g_4}{4}(r - a)^4$  (5)

In Eq. (1),  $a$  is the distance at which the energy is minimum. In Eq. (2),  $a$  is the radius of the hard core elastic repulsion. In Eq. (4),  $\epsilon$  characterizes the intensity of the interaction, and  $\sigma$  is the distance at which the Lennard-Jones (LJ) potential vanishes,  $a = 2^{1/6}\sigma$  being the rest distance at which the potential switches from being repulsive to being attractive. In Eq. (5),  $a$  is the distance at which the  $\beta$ -FPUT force vanishes, *i.e.* the rest distance at which the interaction energy is minimum. The rest distance of the soft-point chain (SPC), *i.e.* the chain with potential (3), is  $a = 1$ . In the LJ case, we also consider first and second nearest neighbour interactions, meaning that they consist of the sum of two terms involving two neighbours, respectively, with characteristic distances  $\sigma$  and  $2\sigma$ :

$$V(r_1, r_2) = 4\epsilon \left[ \left( \frac{\sigma}{r_1} \right)^{12} - \left( \frac{\sigma}{r_1} \right)^6 \right] + 4\epsilon \left[ \left( \frac{2\sigma}{r_2} \right)^{12} - \left( \frac{2\sigma}{r_2} \right)^6 \right] \quad (6)$$

where  $r_1$  is the distance between the particle of interest  $i$  say, and particle  $i + 1$ , and  $r_2$  the distance between particle  $i$  and particle  $i + 2$ . Then, the mechanical equilibrium configuration of the chain is the same produced by the potential (4).

Denoting by  $S_i = \langle r_i \rangle$  the time average of  $r_i = x_{i+1} - x_i$ , *i.e.* of the difference of the coordinates of two particles with consecutive labels (obviously a microscopic quantity), and by  $T_i = \langle p_i^2/2 \rangle$  the time average of the kinetic energy of the particle labelled by  $i$  (another microscopic quantity), Eq. (5) of Ref. [15] can be written as:

$$T_i = c_1 \cdot S_i + c_2, \quad i = 1, \dots, N \quad (7)$$

where  $c_1$  and  $c_2$  are real coefficients that depend on the system under investigation. This relation has been reported to hold in numerous situations, cf. [15–17, 31]. Was  $c_2$  negligible, we would have had a microscopic version of Boyle's law, but in general  $c_2$  is not negligible. The quantities  $S$  and  $T$  can be seen as microscopic extensions of the notions of local inverse density and temperature (apart from the factor  $k_B$ ).<sup>2</sup> In Ref. [32], the equation of state (7) has been derived under the assumption that a functional dependence  $F(S, T) = 0$  of  $S$  and  $T$  exists at each point along the chain, and that  $\Delta T = T_R - T_L$  is small.

Based on the results of Refs. [10, 30], in the present paper, we are going to show that such a derivation does not apply in the case of symmetric potentials, and we develop a more general approach. In particular, we investigate the validity of the equation of state (7) mainly considering 1-dimensional chains of oscillators linked by nearest neighbours interactions. We study the effects of stretching or compressing our chains, which is achieved placing the walls at distances larger or shorter than  $N + 1$  times the rest distance  $a$ . The deformation of the chain is quantified introducing the dilation factor:

$$\alpha = \frac{x_{N+1} - x_0}{a(N+1)}, \quad (8)$$

where  $x_{N+1}$  and  $x_0$  are the fixed positions at the two ends of the chain. In the absence of thermostats, the moving particles oscillate about their mechanical equilibrium positions, expressed by:

$$x_i^{eq} = i a \alpha, \quad i = 1, \dots, N. \quad (9)$$

When  $\alpha = 1$  the chain is neither stretched nor compressed, and the quantity that can be associated with pressure,  $P$  say, depends on the potential, e.g. for  $\beta$ -FPUT,  $\alpha = 1$  corresponds  $P = 0$ . The cases with  $\alpha > 1$  correspond to a stretched chain, called negative pressure states,  $P < 0$ . The cases with  $\alpha < 1$  correspond to compressed chains, of positive pressure,  $P > 0$ . This terminology is motivated by the assumption that the equilibrium statistic of the microscopic phases is given by canonical distributions with a constant parameter  $P$  denoting the pressure, and is justified by the fact that the particles at  $x = 0$  and  $x = (N + 1)a$  are subjected to mean forces that, respectively, pull inside, vanish, or push outside the interval  $[x_0, x_{N+1}]$  they delimit.

We have found that changing  $\alpha$  at fixed  $T_L$  and  $T_R$ , intriguing and unexpected profiles of  $S$  and  $T$  arise, and that the microscopic equation of state (7) robustly holds, except in particular regions of the parameter space, which are wider in the case of the  $\beta$ -FPUT chains than in the other chains we studied. These facts are related to the symmetries of the interaction potentials, which under certain conditions also affect the energy transport as in Refs. [8–10, 10–12, 30], while under other conditions they do not [34, 35]. Omitting to repeat all times that the boundary particles usually do not behave like the bulk particles, our main findings are the following.

Commonly, the  $T$  profile interpolates monotonically between  $T_L$  and  $T_R$ , hence relation (7) can be verified if also  $S$  is monotonic. This is not always the case. For instance, Eq. (7) does not hold for the  $\beta$ -FPUT chains, whose potential is symmetric, when the mechanical equilibrium configuration of the chain constitutes a lattice whose nodes are the rest positions of the potential. In that case, indeed, the  $S$  profile is flat. Differently, in the case of harmonic potentials, which are also symmetric, Eq. (7) holds. The fact is that both  $S$  and  $T$  are flat in the bulk of harmonic chains; hence, Eq. (7) is verified with  $c_1 = 0$  and  $c_2 = T$ . Stretching or compressing the  $\beta$ -FPUT chain, i.e. setting  $\alpha > 1$  or  $\alpha < 1$ , respectively, the situation changes drastically. The rest positions of the particles in the chain do not coincide anymore with  $x_i = ia$ . Consequently, the interaction potential is not symmetric about the mechanical equilibrium positions, the  $S$  profile acquires a slope, and it gradually couples to  $T$  as Eq. (7) prescribes.

For asymmetric potentials, the relation (7) is generally quite robust under parameters variations. The  $\beta$ -FPUT chains are peculiar from this point of view. This may be related to the fact that their potential, while confining particles more strongly than harmonic potentials, lacks a short-range repulsive singularity.

Changing bath temperatures one obtains different  $S$  and  $T$  profiles, with different  $c_1$  and  $c_2$ . Fixing  $T_R$ , these coefficients vary linearly with  $T_L$  up to quite large values, and then they bend toward a nonlinear regime for still higher values. This has been observed to be the case for the  $\beta$ -FPUT, the SPC and the nearest neighbour LJ potentials. The above suggests that Eq. (7) is a nontrivial relation, albeit simple and concerning the two most obvious observables of 1-dimensional particles systems. Symmetries of potentials and equilibrium positions play an enthralling role, here, as they do for energy transport.

As analogous results hold also with stochastic thermal baths, Eq. (7) is suitable to play the role of an equation of state for nonequilibrium (even nonstationary and nonthermodynamic) states of oscillators chains,<sup>3</sup> capable of distinguishing qualitatively different situations for a wide set of 1-dimensional systems. Indeed, with only two microscopic parameters, it characterizes states in a simple fashion, without need for detailed knowledge of the dynamics, like equilibrium thermodynamic equations of state.

We conclude that the case of  $\alpha = 1$ , which is usually investigated, is peculiar also from the point of view of the state equation (7) that qualitatively changes behaviour at that point. In fact, it is reasonable that something happens when pressure changes from positive to negative. Interestingly, reducing temperature jumps or eliminating them, setting  $T_L = T_R$ , does not change this qualitative picture. The validity of Eq. (7) is gradually restored when the asymmetry of the overall interaction potential turns significant.

In the following sections we report our results about systems with the potentials introduced above. The numerical integrator used is the fourth-order Runge–Kutta method with step size  $10^{-3}$ . In most cases the heat baths are modelled by the deterministic

<sup>2</sup> The thermodynamic density and temperature require not only averaging over microscopically very long times, but also averaging over mesoscopic cells occupied by a large number of particles, in which boundary effects are negligible compared to the content of the bulk.

<sup>3</sup> In equilibrium it holds, but trivially.

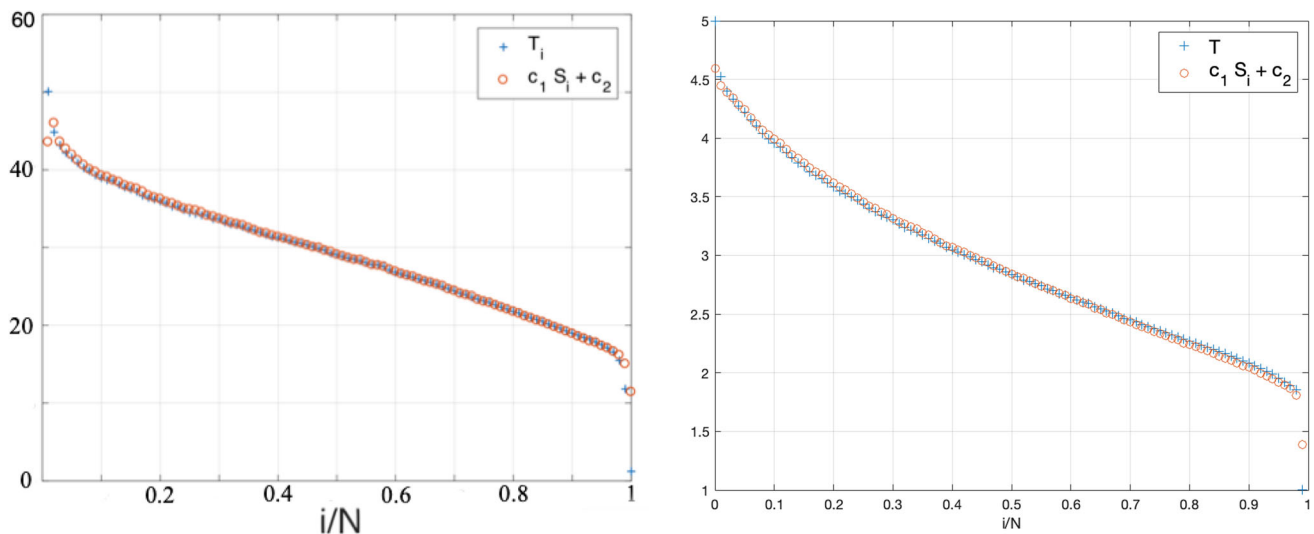


**Fig. 1** Left panel: long-range harmonic potential and short-range hard core repulsion (2) with  $N = 100$  and  $T_L = 50$  and  $T_R = 1$ . In this panel red circles represent the right-hand side of (7). Right panel: verification of relation (7), for SPC chains with  $\alpha = 1$ ,  $T_R = 1$  and  $T_L = 5$ . In both cases, temperature and  $S$  profiles are nontrivially coupled since relation (7) is perfectly verified with  $c_1 > 0$ . This means that density of particles is lower where the kinetic temperature is higher. The values of  $c_2$  are not negligible; therefore, this system does not behave like a perfect gas

Nosé–Hoover thermostat with relaxation time set to 1. However, in order to check the robustness of our results against the modelling of the baths, a stochastic bath is used and described in Subject. 4.2.

### 3 Effect of interaction potentials

The microscopic interaction potentials have limited impact on thermodynamic quantities that concern large systems occupying a 3-dimensional volume. The effect may be observed on a quantitative level for certain variables, but systems characterized by quite different microscopic dynamics enjoy an almost incredible similarity as proven, for instance, by the perfect gas law or by the existence of universality classes. About thermal phenomena, this was concisely and wittily expressed in Ref. [36] even for nonequilibrium macroscopic systems, driven by thermal baths interacting with their surface: “*the properties of a ‘long’ metal bar should not depend on whether its ends are in contact with water or with wine ‘heat reservoirs’*”. Recently these notions have been considered also in the case of anomalous transport phenomena [37], which low-dimensional lattices of oscillators commonly yield. Nevertheless, no fully developed theory is available about such phenomena and systems. Moreover, the nonlocality observed in numerous 1-dimensional systems may amplify the effect of microscopic interactions and affect the validity of certain relations. Therefore, we now investigate the validity of Eq. (7) for different interaction potentials, recalling that potential symmetry or asymmetry at times makes a difference also for transport [10, 30]. In our case, the interaction potential is indeed responsible for different phenomena, which we first illustrate and later interpret theoretically. We begin with the harmonic potential, which is symmetric, and with the nonsymmetric potential obtained adding hard core interactions to the harmonic springs. These potentials may be regarded as two limit cases obtained by deformation of the  $\beta$ -FPUT potential. Later we briefly consider also the Lennard–Jones and the SPC potentials.

#### 3.1 Harmonic and harmonic plus hard core

Consider harmonic potentials with  $\alpha = 1$  and Nosé–Hoover thermostats at  $T_L = 5$  and  $T_R = 1$ . We realize that Eq. (7) is trivially verified, as already observed in Ref. [15] for much larger  $\Delta T$ , because the  $T$  and  $S$  profiles are flat in the bulk of the harmonic chain, and Eq. (7) holds setting  $c_1 = 0$ , and properly fixing  $c_2$ .

If we add hard core repulsion to the harmonic thermostatted chain, see Eq. (2), we find that the  $T$  and  $S$  profiles generally verify Eq. (7), with  $c_1 > 0$ . Then, kinetic temperature and mass distribution are coupled in such a way that the mean distance between particles is higher in the regions of higher kinetic temperature. This is what one would expect for a normal thermodynamic system, when the mean kinetic temperature corresponds to the thermodynamic temperature, and the mean distance between particles can be directly related to the inverse density. In particular, the left panel of Fig. 1 shows the excellent agreement of the data with relation (7) for simulations with  $N = 100$ ,  $\alpha = 1$ , and a relatively large  $\Delta T$  that should not fit the derivation of Ref. [32]. Note that  $c_2$  is large in our simulations, which excludes that the system is considered a perfect gas. Indeed, for a perfect gas the temperature is proportional to the inverse of the density, so  $c_2$  is zero. On the contrary, we note that for a system of many particles,  $N \gg 1$ , and given  $L$ , the average length of the chain,  $c_2$  approximately equals the mean temperature of the chain:

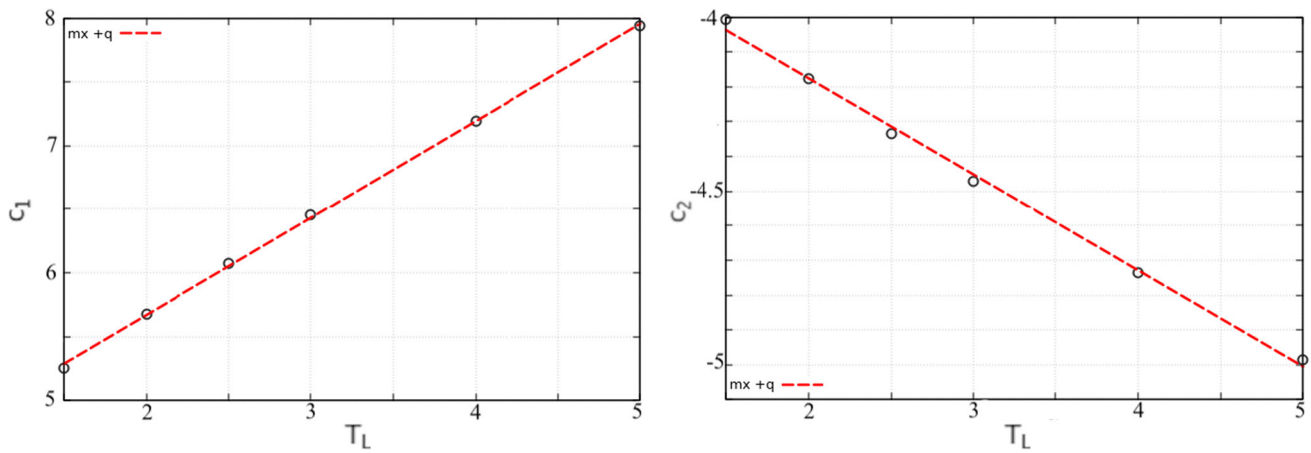


**Fig. 2** Behaviour of  $c_1$  (left) and  $c_2$  (right) with Nosé–Hoover thermostats at  $T_L \in [1.5, 5]$  for SPC chains with  $T_R = 1$ ,  $a = 1$  and  $\alpha = 1$ . The red dashed lines are the linear fit for  $T_L$  up to 5. A linear behaviour is evidenced for relatively small  $T_L$ , which turns nonlinear at higher  $T_L$

$$c_2 \simeq \bar{T} = \frac{1}{N} \sum_{i=1}^N T_i$$

In fact, computing the mean temperature, Eq. (7) yields:

$$\frac{1}{N} \sum_{i=1}^N T_i = \frac{c_1}{N} \sum_{i=1}^N S_i + c_2 = \frac{c_1}{N} L + c_2 \tag{10}$$

which approximately equals  $c_2$  if  $N$  is large compared to  $L$ , *i.e.* if the spacing between particles is small on the scale of the chain.

### 3.2 SPC potential

In the SPC case, Eq. (7) is well verified, for  $\alpha = 1$  with  $c_1 > 0$ , see the right panel of Fig. 1, which means that the density of particles is lower where the kinetic temperature is higher, as normally expected when thermodynamic identifications make sense. This is illustrated by simulations performed for  $N = 100$  and Nosé–Hoover thermostats of temperatures  $T_L = 5$  on the left and  $T_R = 1$  on the right. Further simulations lead to the same results. The behaviour of  $c_1$  and  $c_2$  with  $T_L$  is quite interesting: at small  $T_L$ , they lie on a straight line, which bends at higher  $T_L$ , cf. Fig. 2. The relatively high values of  $c_2$  indicate that this chain does not behave like a perfect gas, if  $S$  and  $T$  are interpreted as thermodynamic quantities.

### 3.3 LJ potential

For the LJ case, the validity of (7) is verified quite generally for  $\alpha = 1$  with  $c_1 > 0$ , as we have observed for  $N = 100, 150$  and  $200$ . As an example, in the right upper panel of Fig. 3 we represent the case  $N = 200$  with first and second nearest neighbour interactions.

Interestingly, although Eq. (7) also performs relatively well, the situation is different for the LJ potential with nearest neighbour interaction only, cf. left upper panel of Fig. 3. Indeed, the  $S$  profile is slightly nonmonotonic, while the  $T$  profile is monotonic, which means that Eq. (7) cannot be exact, but only approximately valid. Nevertheless, this relation remains generally quite accurate, even under mild as well as strong stretching conditions, where  $c_1$  is always positive. For nearest neighbour LJ chains we verified this fact for several values of  $\alpha$  ranging from 1.2 to 100, and we found that relation (7) holds even when the raw data are noisy. This then suggests one further test. In the lower panels of Fig. 3, the profiles are shown for growing times of  $1/4, 1/2$ , and total time  $t_{\max}$  with  $t_{\max} = 8 \cdot 10^5$ . Figure 3 shows that relation (7) is verified also when  $T$  and  $S$  profiles are far from their asymptotic shape.

One further observation for LJ chains is that the  $S$  profile converges to a bounded asymptotic profile  $S^\infty$  as the left reservoir temperature  $T_L$  grows, at fixed  $T_R=1$ . In other words, denoting by  $S_i^{T_L}$  the value of the  $S$  profile at the  $i$ -th site, with left bath at temperature  $T_L$ , and by  $S_i^\infty$  the corresponding asymptotic value, we can write:

$$S_i^{T_L} = S_i^\infty + \delta_{T_L}(i), \quad \text{where } \delta_{T_L}(i) \rightarrow 0 \text{ as } T_L \rightarrow \infty. \tag{11}$$

Relation (7) holds for all  $T_L$ , and our simulations show that its coefficients  $c_1$  and  $c_2$  depend on  $T_L$  and draw a straight line up to quite large values of  $T_L$ . Consequently, the kinetic temperature profile at finite  $T_L$  can be related to the asymptotic  $S$  profile as:

$$T_i = c_1(T_L)S_i^\infty + c_2(T_L) + c_1(T_L)\delta_{T_L}(i). \tag{12}$$



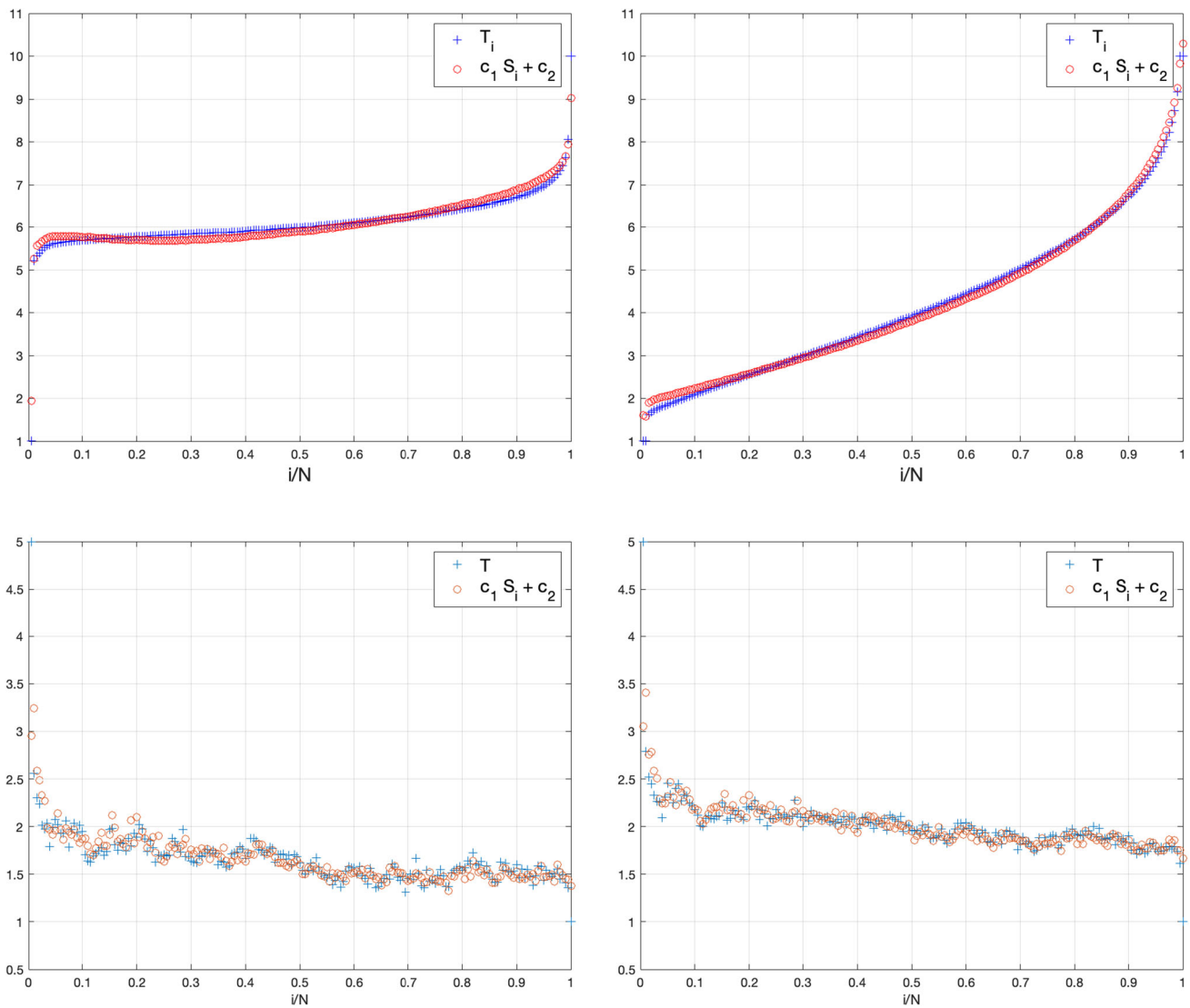


**Fig. 3** Top panels: Relation (7) for LJ chains with nearest neighbour interactions (left panel), and first and second nearest neighbour interactions (right panel).  $N = 200$ ,  $\alpha = 1$ ,  $T_L = 1$  and  $T_R = 10$ . The density profile is not strictly monotonic, which makes Eq. (7) only approximately but reasonably well verified. Bottom panels: LJ chain with nearest neighbour interactions with  $N = 200$ , Nosé–Hoover thermostats at  $T_L = 5$  and  $T_R = 1$ , and  $\alpha = 100$ . Equation (7) is verified even if the averaging times are quite short:  $1/4$  (left panel) and at  $1/2$  (right panel) of the maximum time

In fact, something more can be observed: Fig. 4 shows the validity of an asymptotic form of (7), i.e.:

$$T_i = \hat{c}_1(T_L)S_i^\infty + \hat{c}_2(T_L) \tag{13}$$

where

$$\hat{c}_1(T_L) = \frac{T_L - T_{L0}}{S_1^\infty - S_N^\infty}, \quad \hat{c}_2(T_L) = T_{L0} - \frac{T_L - T_{L0}}{S_1^\infty - S_N^\infty} S_1^\infty. \tag{14}$$

### 4 $\beta$ -FPUT oscillators

Given the wide applicability of the state Eq. (7) revealed by the previous cases, in this section we investigate  $\beta$ -FPUT chains, which are known to be peculiar under various respects. We consider states of the chain at different pressure, generated by different stretching rates  $\alpha$ .

When  $\alpha = 1$ , the chain is neither compressed nor stretched (for any value of  $a$ ). In this case, not only the interaction potential is symmetric with respect to its centre, but this centre coincides with the rest distance for any pair of interacting particles. Consequently,

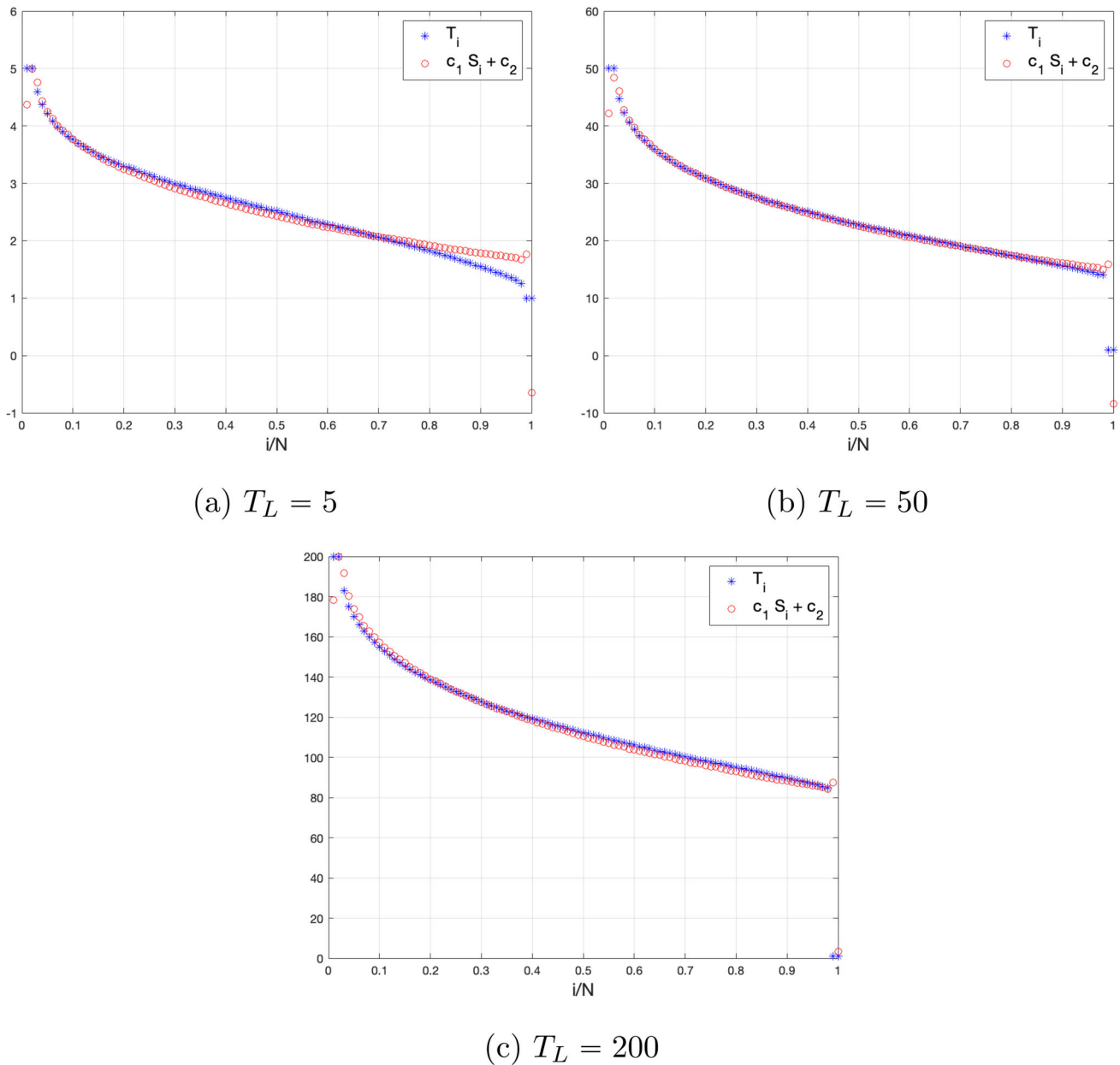


**Fig. 4** LJ chain with  $N = 100$  and  $T_R = 1$ . Equation (13) with coefficients given by Eq. (14) is well verified. The  $S^\infty$  profile is the one obtained at  $T_L = 300$ . Beyond this value, variations of this profile are not appreciable

the forces acting on each particle are symmetric with respect to their mechanical equilibrium positions,  $x_i^{eq}$ , about which particles oscillate if there are no thermostats.

In equilibrium conditions, i.e. if there are thermostats at same temperature acting on particles 1 and  $N$ , the mean distance of particle 1 from particles 0 and 2, and of particle  $N$  from particles  $N - 1$  and  $N + 1$  could be different from the mean distance between consecutive particles in the bulk of the chain. In fact, there would be different forces acting on these particles. On the other hand, physically one expects the symmetry of the potentials about the mechanical equilibrium positions to make equally spaced the bulk particles (that do not interact with thermostatted particles). The kinetic energy of all particles would also be uniform along the chain; therefore, the state Eq. (7) would be trivially verified, i.e. with  $c_1 = 0$ , as usual at equilibrium.

Now, we consider  $\beta$ -FPUT chains with  $a = 1$ ,  $\alpha = 1$ , and Nosé–Hoover thermostats at  $T_R = 1$  and  $T_L = 5$ . Like in the case of harmonic chains studied in Ref. [36], we find that the inverse density profile,  $S$ , is practically flat, with  $S_i = a$ , apart from the region next to the walls and thermostats. This shows that the particles in the bulk oscillate about their mechanical equilibrium positions  $x_i^{eq}$ . Unlike harmonic chains, however, the kinetic temperature profile,  $T$ , monotonically decreases with the particle label  $i$ , interpolating between  $T_L$  and  $T_R$ , cf. Fig. 5. This holds with different bath temperatures, as long  $\alpha = 1$ . In this case, (7) cannot hold because no



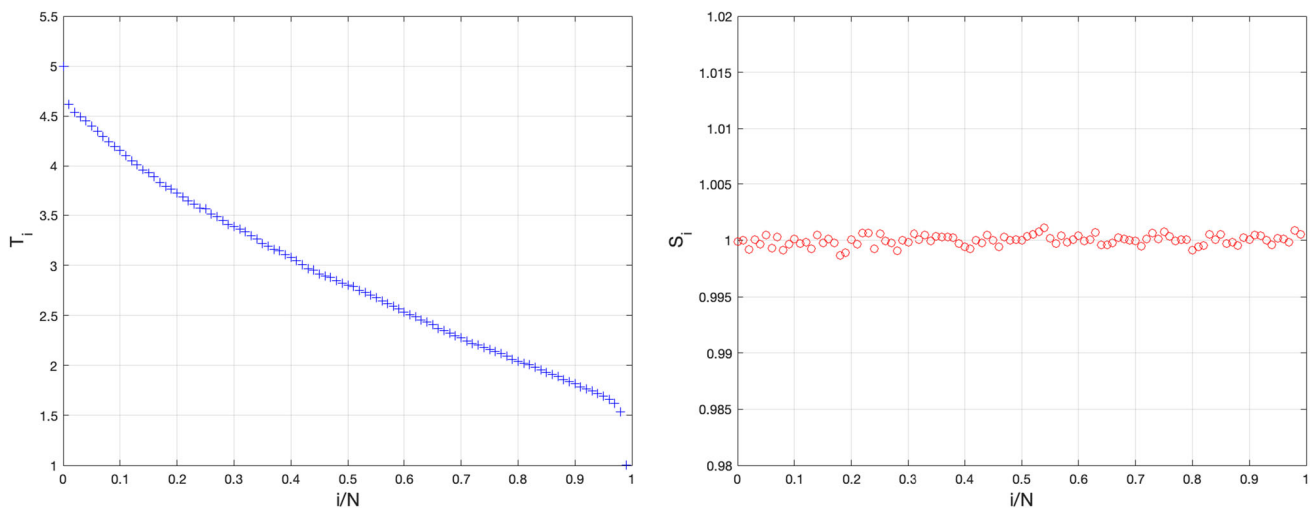


**Fig. 5** Profile of  $T$  (left) and  $S$  (right) for the  $\beta$ -FPUT chain with  $N = 100$ ,  $a = 1$ ,  $\alpha = 1$ ,  $T_L = 5$  and  $T_R = 1$ . The rest distance of particles is positive; hence, they repel each other when they get too close. The length of the chain makes it neither stretched nor compressed, on average. The profile of  $S$  is constant and equal to the equilibrium distance  $a$ , a part from negligible noise, magnified by the scale of the vertical axis

factor  $c_1$  turns the 0 angular coefficient of a horizontal line into a positive one. Consequently, the  $T$  and the  $S$  profiles are decoupled from each other and cannot be related by an equation of state.

Quite unexpectedly, then, the relation  $F(P, S, T) = 0$  of Ref. [32], from which Eq. (7) could be obtained in the limit of small perturbations of the equilibrium state, does not apply, irrespective of the smallness of the perturbation. On the other hand, this is a singular condition that is strictly verified only at  $\alpha = 1$ , as far as simulations demonstrate. It signals that the chain behaviour drastically changes when passing from compressed to stretched.

We argue that such facts are consequence of the symmetry about the equilibrium positions of the forces acting on the oscillators. Symmetry tends to preserve the uniformity of the distribution of particles, as much as allowed by the contrasting effects of the boundary conditions.

As a matter of fact, the scenario changes for  $\alpha \neq 1$ , when the mechanical equilibrium positions (9) do not coincide anymore with the rest positions of the interaction potential, which are points of symmetry for that potential.<sup>4</sup> Then, the forces acting on the particles appear generated by nonsymmetric potentials that contribute to break the spatial uniformity of the distribution of particles. The  $S$  and  $T$  profiles may then be coupled, and various possibilities arise.

For  $\alpha < 1$ , the chain is compressed, at “equilibrium” the pressure is positive, the gradients of the  $T$  and  $S$  profiles have same sign, and the constant  $c_1$  is positive. This means that density is lower where the chain is hotter, which seems to be a normal condition. However, the relation (7) is not perfectly verified for  $\alpha = 0.5$  and  $0.8$ , as top row of Fig. 6 shows.

Like under compression, Eq. (7) is only approximately verified when the chain is mildly stretched. Results from simulations with  $a = 1$  and  $\alpha = 1.2$  and  $1.5$  are reported in bottom row of Fig. 6. We may regard the range  $1 < \alpha < 2$  analogous to  $0 < \alpha < 1$  for shifting (with opposite sign) the chain mechanical equilibrium positions with respect to the rest positions of the interaction potential. Indeed, a similar performance of the linear relation is obtained. What matters is how much  $\alpha$  differs from 1, whether larger or smaller. Note the similarity of the cases with  $\alpha = 0.8$  and  $1.2$ , and that of the cases with  $\alpha = 0.5$  and  $1.5$ . Relation (7) improves as  $|1 - \alpha|$  grows; cf. left panel of the top row of Fig. 6, concerning the case  $\alpha = 0.5$  and  $0.8$ , with those of the top row of Fig. 6, for  $\alpha = 1.2$  and  $1.5$ .

Figure 7 provides an overview of the behaviour of the weakly deformed chain. As  $\alpha$  departs from 1, growing or decreasing is the same, the mechanical equilibrium positions depart from the points of symmetry of the interaction potentials, and monotonic  $S$  profiles, which can be coupled with the monotonic profiles of  $T$ , immediately emerge: this appears to be a discontinuous nonequilibrium transition. Consequently, the linear relation (7) becomes verified, with varying degrees of accuracy.

As  $c_1$  and  $c_2$  depend on the baths temperatures, it is interesting to study how they are related to each other. Having fixed  $T_R$  we have found the same behaviour observed for SPC and LJ, see Sects. 3.2 and 3.3, i.e. that both coefficients depend linearly on  $T_L$  at least up to a certain value, and then the dependence turns nonlinear at higher  $T_L$ .

#### 4.1 Effects of symmetry of potentials

As reported in Sect. 4, the particles of the  $\beta$ -FPUT model, which has symmetric interaction potential, do not shift their mean position, even in presence of a temperature gradient, when the system is at its rest length ( $\alpha = 1$ ). However, if we stretch or

<sup>4</sup> The case  $a = 0$  means that the chain is always stretched and, indeed, we have found the same results obtained with  $\alpha > 1$ ; hence, we do not report them.

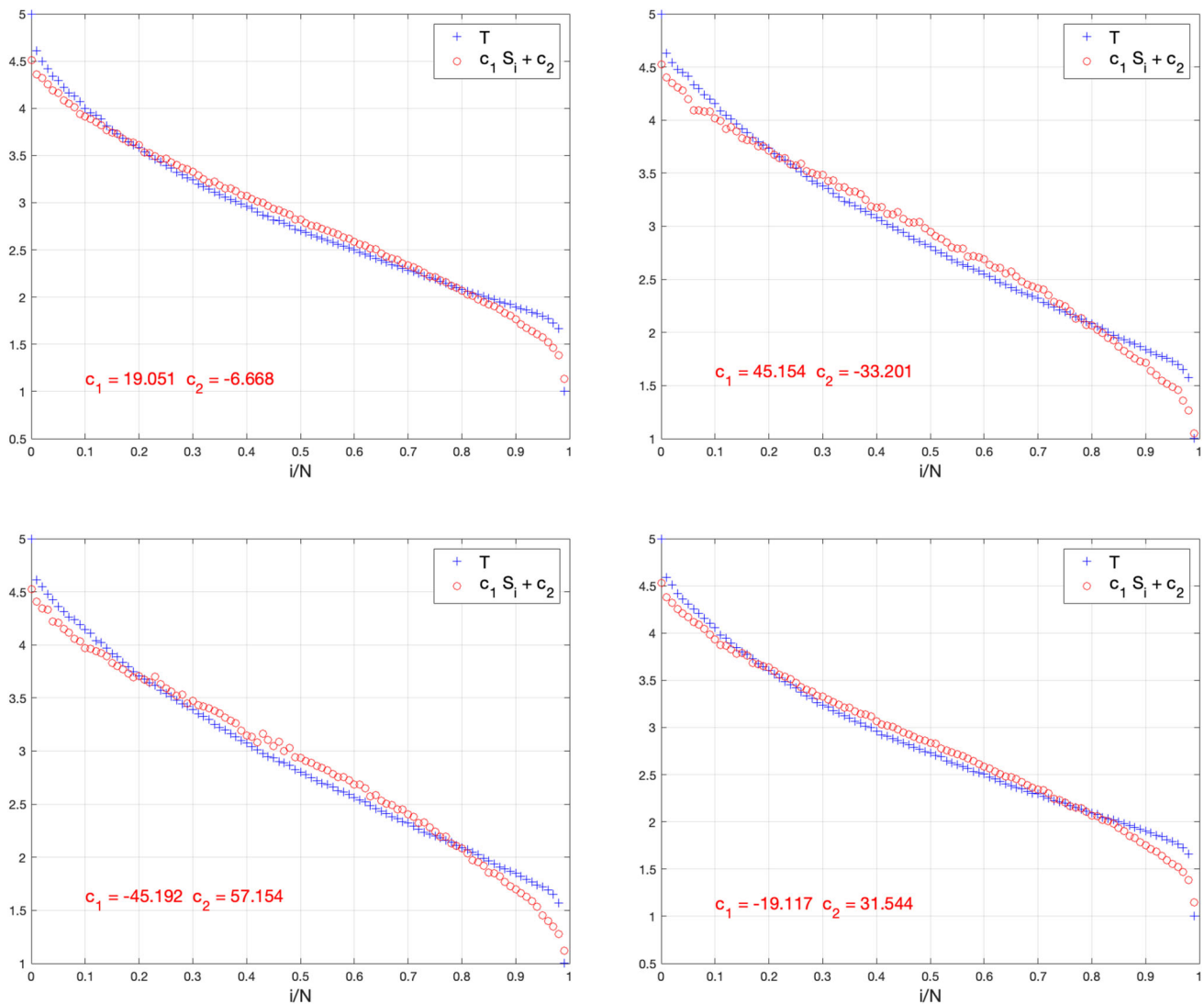


**Fig. 6**  $\beta$ -FPUT chain with  $N = 100$ ,  $\alpha = 1$ , and Nosé–Hoover thermostats at  $T_L = 5$  and  $T_R = 1$ . Top row: the chain is compressed with  $\alpha = 0.5$  (left) and  $\alpha = 0.8$  (right). Bottom row: the chain is stretched with  $\alpha = 1.2$  (left) and  $\alpha = 1.5$  (right). Equation (7) is better verified when  $\alpha$  differs more from 1. Note the similarity of top left panel with bottom right panel, and of top right panel with bottom left panel. Under compression  $c_1$  is positive. Under stretching it is negative

compress the chain, a mass gradient develops and can be coupled to the  $T$  profile. Moreover, some behaviour transition takes place as the stretching grows.

To understand why this happens, we have investigated the interactions change that particles perceive under stretching. For the sake of definiteness we consider half of the potential acting on the generic  $i$ -th particle, i.e.:

$$V(r) = \frac{(r - a)^2}{2} + \frac{(r - a)^4}{4}, \tag{15}$$

where  $r = r_i = x_{i+1} - x_i$  and  $a$  is the rest length of the spring. When the chain is neither stretched nor compressed ( $\alpha = 1$ ), the mechanical equilibrium is expressed by  $x_i^{eq} = ia$ . In this case, the potential  $V$  is symmetric with respect to the mechanical equilibrium distance  $r = r^{eq} = a$ , and the density profiles are flat, in accord with the numerical data shown in Fig. 5.

If we stretch the chain by a factor  $\alpha > 1$ , so that the distance between the two fixed particles at the ends of the chain is  $\alpha(N + 1)a$ , the new equilibrium configuration is given by  $\hat{x}_i^{eq} = i\alpha a \equiv i(a + d)$ , where  $d = a(\alpha - 1)$  is the distance between the stretched and the rest equilibrium positions. In this situation the particles oscillate about  $\hat{x}_i^{eq}$  and the displacements  $r_i$  oscillate about  $r = \hat{r}^{eq} = a + d$ , which is neither a point of symmetry nor a minimum of  $V$ , see Fig. 8. Let us examine the effect of this asymmetry as the chain is stretched, and the vertical axis  $r = \hat{r}^{eq}$  in Fig. 8 is moved to the right of  $r = a$  (corresponding to  $d = 0$ ).

In order to focus on the new equilibrium displacement  $\hat{r}^{eq} = a + d$  we rewrite the potential  $V$  setting  $r = \hat{r}^{eq} + z$  in (15), which yields:

**Fig. 7**  $\beta$ -FPUT chain with  $N = 100, a = 1$ , and Nosé–Hoover thermostats at  $T_R = 1$  and  $T_L = 5$ , and different values of  $\alpha$ , in the interval  $[0.2, 2]$ . The sudden change of  $c_1 S_i + c_2$ , when  $\alpha$  decreases or increases away from 1 is shown. For  $\alpha = 1$ , since the relation (7) does not work, we put  $c_1 = 0$  and  $c_2 = (T_L + T_R)/2 = 3$

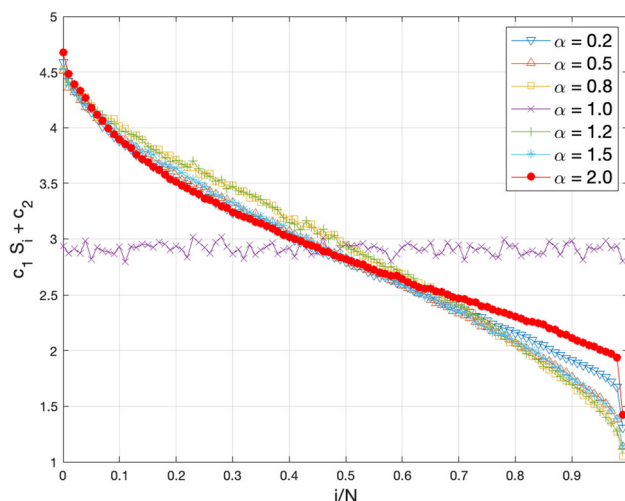
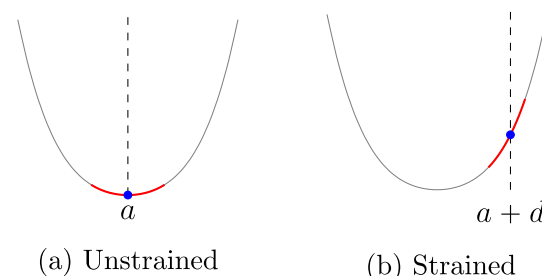


**Fig. 8** Under stretching the vertical axis indicating the equilibrium position is moved to the right



$$V(r) \equiv V(\hat{r}^{eq} + z) = \frac{d^2}{2} + \frac{d^4}{4} + \tilde{V}_\alpha(z)$$

with

$$\tilde{V}_\alpha(z) = \mathbf{a}_1 z + \mathbf{s}_2 z^2 + \mathbf{a}_3 z^3 + \mathbf{s}_4 z^4, \tag{16}$$

where

$$\mathbf{a}_1 = d(1 + d^2), \mathbf{s}_2 = \frac{1}{2}(1 + 3d^2), \mathbf{a}_3 = d, \mathbf{s}_4 = \frac{1}{4}.$$

The subscript  $\alpha$  in (16) refers to the fact that the coefficients of the polynomial  $\tilde{V}_\alpha(z)$  via  $d$  depend on  $\alpha$ . Indeed, the coefficients of the asymmetric terms (odd powers) in  $\tilde{V}_\alpha(z)$  are:

$$\mathbf{a}_1 = a(\alpha - 1)(1 + a^2(\alpha - 1)^2), \quad \mathbf{a}_3 = a(\alpha - 1),$$

and those of the symmetric one (even powers) are

$$\mathbf{s}_2 = \frac{1}{2}(1 + 3a^2(\alpha - 1)^2), \quad \mathbf{s}_4 = \frac{1}{4}.$$

Obviously, the asymmetric coefficients vanish for  $\alpha = 1$ . Thus, in the case of a slightly stretched chain (*i.e.* for  $\alpha \approx 1$ )  $\tilde{V}_\alpha(z)$  is a small perturbation of the original symmetric potential that still dominates the dynamics. In the opposite limit, *i.e.* for a large stretching of the chain ( $\alpha \gg 1$ ) the terms in the potential with the largest coefficients are the harmonic and the first-order anharmonic ones, with  $\mathbf{a}_1 \sim a^3(\alpha - 1)^3$ . More precisely, consider that anharmonic interactions are required for nonconstant temperature profiles to be established, and that fluctuations of positions can be relatively large, *e.g.*  $O(1)$ . Then, for  $a = 1$  or larger, we have the following:

1. For a stretching factor  $\alpha = 1 + \delta$  with  $0 < \delta \ll 1$ , (*i.e.* small  $d > 0$ ),  $\mathbf{a}_1, \mathbf{a}_3 = O(\delta)$  and  $\mathbf{s}_2, \mathbf{s}_4 = O(1)$ , then the nonlinear interaction is dominated by the symmetric potential terms  $\mathbf{s}_2 z^2 + \mathbf{s}_4 z^4$  and, as in the case of  $\beta$ -FPUT with  $\alpha = 1$ , relation (7) fails.
2. For  $\alpha \approx 1.5$  (*i.e.*  $d \approx 0.5$ ), and deviations  $z = O(1)$  from equilibrium, the amplitudes of symmetric and asymmetric terms, *i.e.*  $\mathbf{s}_2 z^2 + \mathbf{s}_4 z^4$  and  $\mathbf{a}_1 z + \mathbf{a}_3 z^3$ , are of the same order (since the coefficients in (16) do the same) and the relation is only approximately satisfied (Fig. 6).

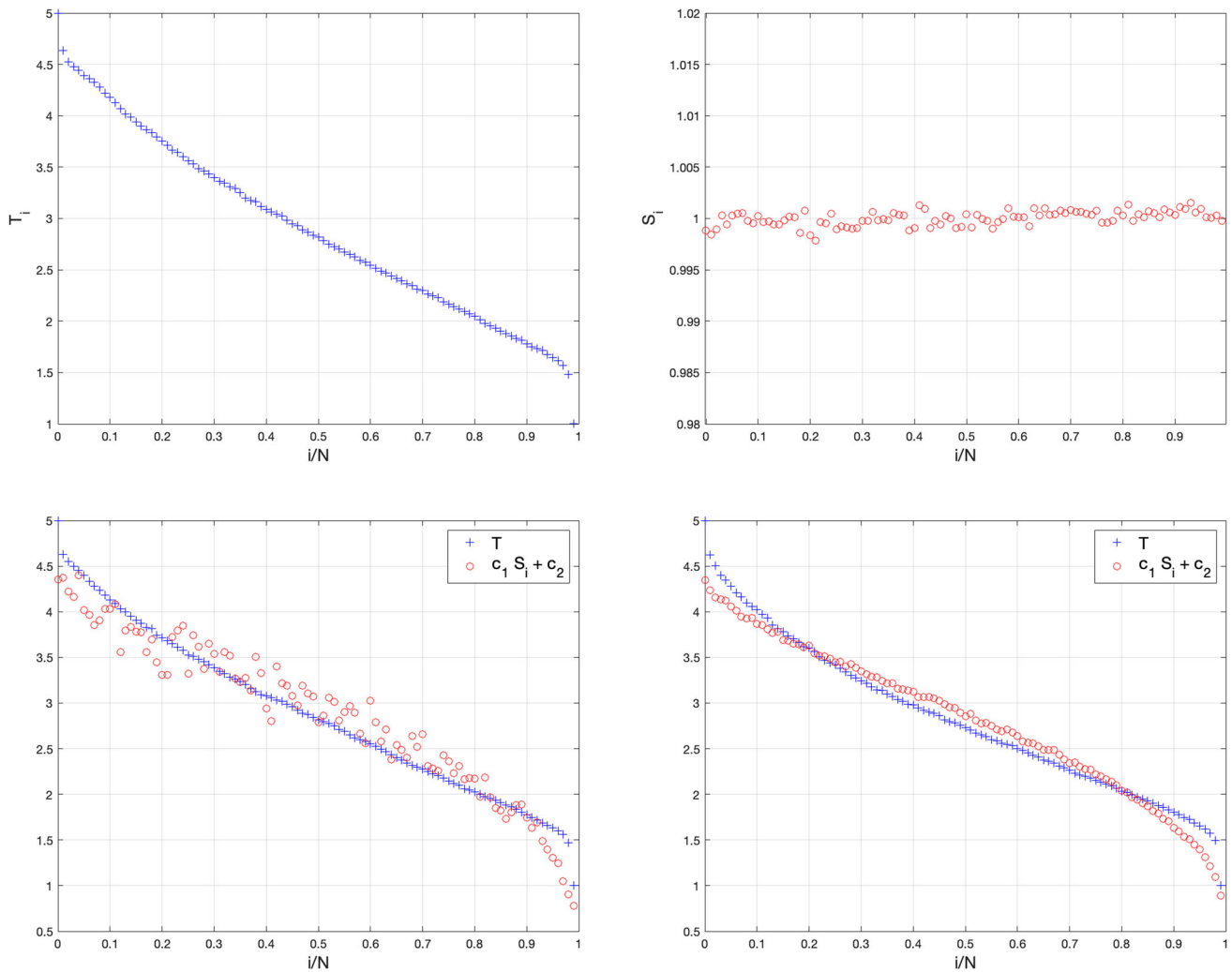


**Fig. 9** Top panels: the profiles of  $T$  and  $S$  for the chain with interacting potential (17) and  $g_3 = 0.01$ ,  $N = 100$ ,  $a = 1$   $\alpha = 1$ ,  $T_L = 5$ ,  $T_R = 1$ . In this case, the rest distance of particles is positive; hence, particles repel each other when they get too close. However, even in the presence of a (small) cubic perturbation of the  $\beta$ -FPUT potential, the length of the chain makes it neither stretched nor compressed, on average. The profile of  $S$  is constant and equal to the equilibrium distance  $a$ , a part from negligible noise. Bottom panels: Linear relation (7) for the chain with interacting potential (17) and with  $N = 100$ ,  $a = 1$   $\alpha = 1$ ,  $T_L = 5$  and  $T_R = 1$ . The coefficient of the cubic term of the potential is  $g_3 = 0.1$  in the left panel and  $g_3 = 1.0$  in the right one

3. For  $\alpha \approx 2$  (i.e.  $d \approx 1$ ), and  $z = O(1)$ , the asymmetric nonlinear term becomes relevant. Indeed,  $a \geq 1$  implies  $\mathbf{a}_1 \geq \mathbf{s}_2$ ,  $\mathbf{s}_4$  and the law (7) is almost perfectly satisfied (Fig. 7).
4. For  $\alpha \gg 2$ , we have  $\mathbf{a}_1 > \mathbf{s}_2 > \mathbf{a}_3 > \mathbf{s}_4$  and, though the harmonic term is still dominant, the cubic term becomes increasingly important, since the coefficient of the quartic term  $\mathbf{s}_4$  remains unchanged and equal to  $1/4$ . In this regime the particles become peculiarly correlated with each other and with the thermostats. Simulations in this regime are numerically challenging, so the possible results have to be further investigated.

We conclude that asymmetric interactions, whichever way they are generated, allow the validity of the equation of state (7), as long as they are not negligible.

This reasoning is consistent with simulations of a chain with this potential:

$$V(r) = \frac{g_2}{2}(r - a)^2 + \frac{g_3}{3}(r - a)^3 + \frac{g_4}{4}(r - a)^4, \tag{17}$$

where  $g_2 = g_4 = 1$  are constants and we study the validity of (7) modifying  $g_3$ . As we can see in top panels of Fig. 9, for  $g_3 = 0.01$  the asymmetric term is totally dominated by the symmetric ones and the linear relation (7) is not satisfied. However, increasing the coefficient of the cubic term we can observe that the relation is better and better satisfied, cf. bottom panels of Fig. 9. Therefore, the mass gradient couples with the temperature gradient when the asymmetric term is not negligible, compared to the symmetric ones.

### 4.2 Stochastic baths

One may wonder whether the above results are due to the known peculiar nature of the Nosé–Hoover thermostat in 1-dimensional systems. As a matter of fact, the detailed structure of our results is affected by the thermal bath model, unlike what happens in real 3-dimensional thermodynamic systems, [15]. However, qualitatively they remain the same if the Nosé–Hoover thermostats are replaced by stochastic baths. Following Ref. [28], we implement such baths by simulating the elastic collisions of particles 1 and  $N$  with virtual Maxwellian bath particles at temperatures  $T_L$  and  $T_R$ , see Eqs. (41) and (42) of [28]. Moreover, the random number  $k$  of discrete time steps between two consecutive collision of a particle with the bath is assumed to have a geometric distribution:

$$P(k) = h(1 - h)^{k-1}, \tag{18}$$

where  $h = \gamma dt$ ,  $dt$  is the time step, and  $\gamma$  is a positive parameter such that  $\gamma dt \leq 1$ , which determines the rate of interaction.

For  $\beta$ -FPUT with  $T_R = 1$ ,  $T_L = 5$  and  $dt = 10^{-3}$ , we then varied  $\alpha$  and  $\gamma$ , obtaining the following results:

$\alpha = 0.5$ ) Equation (7) holds with  $c_1 > 0$ , and thermostat efficiencies  $\gamma = 10$ , cf. Fig. 10a.

$\alpha = 1$ )  $T$  profile monotonically decreases, while  $S$  profile is flat for  $\gamma = 10$ , cf. Fig. 10b. In this case, Eq. (7) does not work; density gradient and temperature gradients are decoupled.

$\alpha = 2$ )  $T$  and  $S$  profiles have opposite trend, so the linear relation is verified with  $c_1 < 0$ . See Fig. 10c for  $\gamma = 10$ .

### 5 Two-dimensional lattice

We briefly mention that an extension to 2-dimensional systems of Eq. (7) also holds. In this case, we consider a network with particles in positions  $\mathbf{r}(i, j)$ ,  $i = 1, \dots, n_y$ ,  $j = 1, \dots, n_x$  in the plane  $(x, y)$ . We have nearest neighbour harmonic interactions, with vanishing rest length, which means that the springs joining the particles are stretched. Then, particle labelled by  $(i, j)$  interact with particles labelled by  $(i, j + 1)$ ,  $(i - 1, j)$ ,  $(i, j - 1)$  and  $(i + 1, j)$ . The boundary particles  $\mathbf{r}(1, j)$ ,  $\mathbf{r}(n_y, j)$ ,  $\mathbf{r}(i, 1)$ ,  $\mathbf{r}(i, n_x)$ ,  $i = 1, \dots, n_y$ ,  $j = 1, \dots, n_x$  interact with wall particles that are at rest so that the positions  $\mathbf{r}^{eq}(i, j) = (a_i, a_j)$  constitute the mechanical equilibrium configuration of the net. The particles on the left (L),  $\mathbf{r}(i, 1)$ , also interact with a Nosé–Hoover thermostat at temperature  $T_L$ ; those on the right (R),  $\mathbf{r}(i, n_x)$ , with a thermostat at temperature  $T_R$ . The kinetic temperature is defined by

$$T_{ij} = \langle v_{ij}^2 \rangle, \tag{19}$$

where  $v_{ij} = \frac{d\mathbf{r}(i,j)}{dt}$  is the velocity of particle  $(i, j)$ , while by inverse average distance of neighbouring particles around the particle labelled by  $(i, j)$  we mean:

$$\langle S_{ij} \rangle = \frac{1}{4} \langle |\mathbf{r}(i, j + 1) - \mathbf{r}(i, j)| + |\mathbf{r}(i - 1, j) - \mathbf{r}(i, j)| + |\mathbf{r}(i, j - 1) - \mathbf{r}(i, j)| + |\mathbf{r}(i + 1, j) - \mathbf{r}(i, j)| \rangle. \tag{20}$$

Our simulations show that, as common in 1-dimensional cases, the kinetic temperature in the centre of the lattice gets higher than at the thermostatted boundaries.<sup>5</sup> On the other hand, unlike the one-dimensional temperature profile of the harmonic system, in the two dimensional one  $T_{ij}$  may be not flat in the bulk.

Now, we rewrite Eq. (7) for the particles labelled by  $(i, j)$  as:

$$\langle v_{ij}^2 \rangle = c_1 \rho_{ij}^{-1} + c_2, \tag{21}$$

where  $\rho_{ij}$  is the average density at  $(i, j)$ . Because in two dimensions one may take  $\rho_{ij}$  as proportional to the inverse of a square distance, i.e.  $\rho_{ij} \propto \langle S_{ij} \rangle^{-2}$ , we obtain:

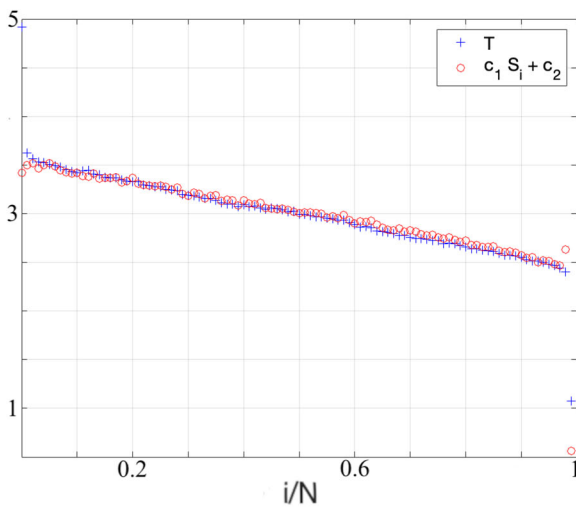
$$\langle v_{i,j}^2 \rangle = c_3 \langle S_{ij} \rangle^2 + c_4. \tag{22}$$

This prediction is confirmed by a numerical quadratic fit. We do not mention any other details here, except that an example in which (22) can be verified is, for instance, a  $20 \times 20$  lattice with  $T_L = 10$  and  $T_R = 1$ .

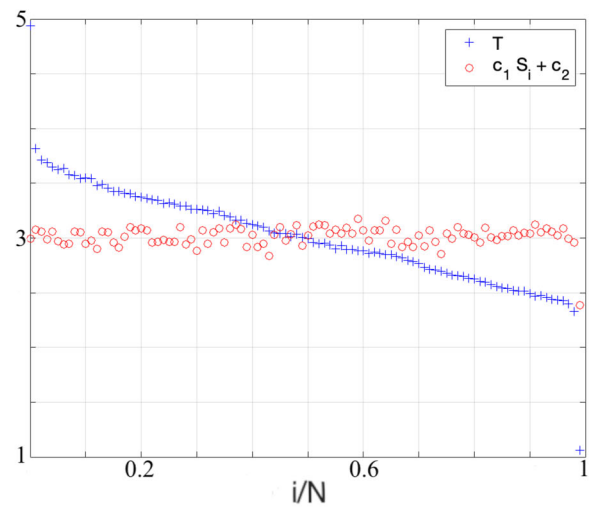
### 6 Concluding remarks

In this paper we have shown that Eq. (7) holds quite widely, and can be considered a state equation for 1-dimensional chains of oscillators. Was  $c_2$  negligible, we would have had Boyle’s law, but in general  $c_2$  is not negligible, and it even gets larger for larger temperature jumps. This characterizes a nonstandard state of aggregation of matter.

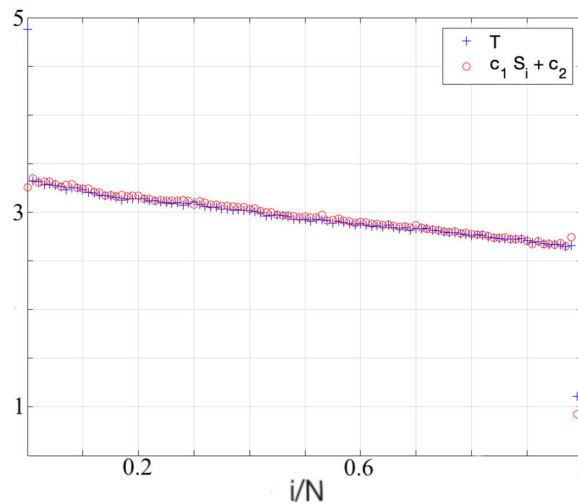
<sup>5</sup> For instance, such a behaviour i.e.  $T_i > \max\{T_L, T_R\}$ , can be observed in the bulk of a stretched 1-dimensional  $\beta$ -FPUT model with  $N = 100$ ,  $T_L = 5$ ,  $T_R = 1$  and  $\alpha > 3.5$ .



(a)  $\gamma = 10, \alpha = 0.5$



(b)  $\gamma = 10, \alpha = 1.0$



(c)  $\gamma = 10, \alpha = 2.0$

**Fig. 10** FPUT chain with  $N = 100, T_L = 5$  and  $T_R = 1$ , with stochastic baths. Top panels: stretching factor is  $\alpha = 0.5$ . Centre panels:  $\alpha = 1.0$ , *i.e.* there is neither compression nor stretching. Bottom panels: stretching factor is  $\alpha = 2.0$

In certain regions of the parameter space, Eq. (7) fails, especially for the  $\beta$ -FPUT potential. In particular, Eq. (7) does not hold in  $\beta$ -FPUT chains when the mechanical equilibrium configuration of the chain constitutes a lattice whose nodes lie in the rest positions of the interaction potential, which is symmetric with respect to such positions. In that case,  $T$  is monotonic, thanks to the presence of nonlinear interactions, but  $S$  remains flat; hence, the two profiles cannot be matched by a relation like (7).

The  $\beta$ -FPUT chains are peculiar, because their potential is symmetric, it confines particles more strongly than harmonic potentials, and it does not preserve their initial order. Nevertheless, this failure carries information about a significant change of behaviour, associated with a change of sign of pressure: in a range of values of the dilatation factor  $\alpha$  around 1, the pressure is nonzero, and Eq. (7) holds.

In the harmonic cases, Eq. (7) is verified because both  $S$  and  $T$  profiles are flat; therefore, it suffices to take  $c_1 = 0$  and  $c_2 = T$ .

For nonlinear interactions, the  $T$  profile typically interpolates monotonically between  $T_L$  and  $T_R$ , and  $S$  is monotonic, in such a way that values  $c_1$  and  $c_2$  can be found for Eq. (7) to represent the data. This is the case of the harmonic+hard core, LJ and SPC potentials. As changing bath temperatures one obtains different  $S$  and  $T$  profiles,  $c_1$  and  $c_2$  change too. The question is whether they follow any rule. As a matter of fact, they vary linearly with  $T_L$  up to quite large values of the difference  $T_L - T_R$ , and then they bend toward a nonlinear regime for still higher values. This has been observed to be the case for the  $\beta$ -FPUT, the SPC and the nearest neighbour LJ potentials. Furthermore, Eq. (7) holds even under time averaging not sufficient to yield the stationary state  $S$  and  $T$  profiles. This fact further shows that Eq. (7) goes beyond a thermodynamic law.



Noteworthy is the behaviour under compression or extension of the chains. The  $\beta$ -FPUT cases, in particular, present a variety of situations, in which the applicability of Eq. (7) alternates. Stretching or compressing the chain, the equilibrium positions of the particles in the chain shift with respect to the minimum of the pair interaction potential. Consequently, the particles in the bulk of the chain are subjected to potentials that appear symmetric or asymmetric, depending on the (a)symmetry of the interaction potential. The (a)symmetry depends on the stretching parameter  $\alpha$ : changing  $\alpha$ , the potential about the mechanical equilibrium positions changes from being dominated by its quadratic term, which is symmetric and not capable of producing a monotonic  $T$  profile, to being sensibly asymmetric, thanks to the linear and cubic terms. This is accompanied by transition regions in the range of  $\alpha$ , in which the state Eq. (7) holds, to regions in which it does not. Such variations of behaviour occur because the volume (or inverse density) gets at times decoupled from the temperature.

In particular, varying  $\alpha$ , flat  $S$  profiles acquire a slope, and gradually couple to the  $T$  profile via relation (7). The respective gradients have same sign, hence  $c_1 > 0$ , when  $\alpha < 1$ , *i.e.* positive pressure, while they have opposite sign, hence  $c_1 < 0$ , when  $\alpha > 1$ , *i.e.* negative pressure. Consequently, the applicability of Eq. (7) changes.

Notably, the linear state equation linking temperature and inverse density holds also in 2-dimensional systems, once the density is properly defined, considering that volume corresponds to squared distances, cf. Eqs (21) and (22).

The above suggests that Eq. (7) is a nontrivial relation, although simple and concerning the two most obvious observables of particles systems. It appears suitable to play the role of an equation of state for equilibrium (where it holds trivially) and nonequilibrium (even nonstationary and nonthermodynamic) states of oscillators networks. It distinguishes qualitatively different situations, for a wide set of systems. It characterizes states in a simple fashion, involving a small set of parameters, without detailed knowledge of the dynamics, as required of usual equilibrium thermodynamic equations of state, although it strictly is a microscopic relation.

**Acknowledgements** V. Di Florio, C. Giberti and L. Rondoni are members of Gruppo Nazionale di Fisica Matematica (GNFM) of Istituto Nazionale di Alta Matematica (INdAM). C. Giberti is member of Centro Interdipartimentale En &Tech and Centro Interdipartimentale Intermech Mo.Re., University of Modena and Reggio Emilia, Italy.

**Funding** Open access funding provided by Politecnico di Torino within the CRUI-CARE Agreement. Funding was provided by Ministero dell'Università e della Ricerca (Grant number: P2022Z7ZAJ).

**Data availability** The data can be request to the corresponding author.

**Open Access** This article is licensed under a Creative Commons Attribution 4.0 International License, which permits use, sharing, adaptation, distribution and reproduction in any medium or format, as long as you give appropriate credit to the original author(s) and the source, provide a link to the Creative Commons licence, and indicate if changes were made. The images or other third party material in this article are included in the article's Creative Commons licence, unless indicated otherwise in a credit line to the material. If material is not included in the article's Creative Commons licence and your intended use is not permitted by statutory regulation or exceeds the permitted use, you will need to obtain permission directly from the copyright holder. To view a copy of this licence, visit <http://creativecommons.org/licenses/by/4.0/>.

## References

1. E. Fermi, P. Pasta, S. Ulam, M. Tsingou, *Studies of nonlinear problems* (Los Alamos National Lab, Los Alamos, NM, US, 1955)
2. G. Gallavotti (ed.), *The Fermi-Pasta-Ulam problem: a status report, Lecture Note in Physics*, vol. 728 (Springer, Berlin Heidelberg, 2008)
3. S. Lepri (ed.), *Thermal Transport in Low Dimensions: From Statistical Physics to Nanoscale Heat Transfer, Lecture Notes in Physics*, Springer (2016)
4. G. Benettin, A. Ponno, Time-scales to equipartition in the Fermi-Pasta-Ulam problem: finite-size effects and thermodynamic limit. *J. Stat. Phys.* **144**(4), 793–812 (2011)
5. M. Onorato, L. Vozella, D. Proment, Y.V. Lvov, Route to thermalization in the  $\alpha$ -Fermi-Pasta-Ulam system. *PNAS* **112**(14), 4208–4213 (2015)
6. Y.L. Lvov, M. Onorato, Double scaling in the relaxation time in the  $\beta$ -Fermi-Pasta-Ulam-Tsingou model Lvov Yuri V and Onorato Miguel. *Phys. Rev. Lett.* **120**(14), 144301 (2018)
7. Z. Wang, W. Fu, Y. Zhang, H. Zhao, Wave-turbulence origin of the instability of Anderson localization against many-body interactions. *PRL* **124**(18), 186401 (2020)
8. CW. Chang, Non-diffusive Thermal Conduction in One-dimensional Materials., *AAPPS Bulletin*, **28**(6), (2018)
9. I.-L. Chang, C.-S. Li, G.-S. Wang, C.-L. Wu, C.-W. Chang, Does equilibrium or nonequilibrium molecular dynamics correctly simulate thermal transport properties of carbon nanotubes? *Phys. Rev. Mater.* **4**(3), 036001 (2020)
10. Y. Zhong, Y. Zhang, J. Wang, H. Zhao, Normal heat conduction in one-dimensional momentum conserving lattices with asymmetric interactions. *Phys. Rev. E* **85**(6), 060102 (2012)
11. S. Chen, Y. Zhang, J. Wang, Jiao, H. Zhao, Key role of asymmetric interactions in low-dimensional heat transport. *JSTAT* **2016**(3), 033205 (2016)
12. S. Lepri, R. Livi, A. Politi, Too close to integrable: crossover from normal to anomalous heat diffusion. *Phys. Rev. Lett.* **125**(4), 040604 (2020)
13. S.R. De Groot, P. Mazur, *TextitNon-Equilibrium Thermodynamics* (Dover Publications, New York, 1984)
14. P.I. Hurtado, Breakdown of hydrodynamics in a simple one-dimensional fluid. *Phys. Rev. Lett.* **96**(1), 010601 (2006)
15. C. Giberti, L. Rondoni, Anomalies and absence of local equilibrium, and universality, in one-dimensional particles systems. *Phys. Rev. E* **83**(4), 041115 (2011)
16. C. Giberti, L. Rondoni, C. Vernia, Temperature and correlations in 1-dimensional systems. *EPJST* **228**(1), 129–142 (2019)
17. C. Giberti, L. Rondoni, C. Vernia,  $O(N)$  fluctuations and lattice distortions in 1-dimensional systems. *Front. Phys.* **7**, 180 (2019)
18. L.D. Landau, E.M. Lifshitz, E.M. *Statistical Physics, part 1*, Pergamon, New York (1980)
19. S. Chibbaro, L. Rondoni, A. Vulpiani, *Reductionism, Emergence and Levels of Reality, The Importance of Being Borderline* (Springer-Verlag, 2014)



20. D. Kondepudi, I. Prigogine, *Modern Thermodynamics: From Heat Engines to Dissipative Structures* (John Wiley & Sons, 2014)
21. H. Spohn, *Large Scale Dynamics of Interacting Particles* (Springer-Verlag, 1991)
22. J. Bellissard, Coherent and dissipative transport in aperiodic solids: an overview. *Dyn. Dissipation* **413–485**, 1 (2002)
23. H.J. Kreuzer, *Nonequilibrium Thermodynamics and Its Statistical Foundations* (Clarendon Press, 1981)
24. M. Falcioni, L. Palatella, S. Pigolotti, L. Rondoni, A. Vulpiani, Initial growth of Boltzmann entropy and chaos in a large assembly of weakly interacting systems. *Phys. A Stat. Mech. Appl.* **385**(1), 170–184 (2007)
25. L. Rondoni, S. Pigolotti, On  $\Gamma$ - and  $\mu$ -space descriptions: Gibbs and Boltzmann entropies of symplectic coupled maps. *J. Phys. Scr.* **86**(5), 058513 (2012)
26. G. Dematteis, L. Rondoni, D. Proment, F. De Vita, M. Onorato, Coexistence of ballistic and fourier regimes in the  $\beta$  Fermi-Pasta-Ulam-Tsingou Lattice. *Phys. Rev. Lett.* **125**(2), 024101 (2020)
27. B. Hu, B. Li, H. Zhao, Heat conduction in one-dimensional chains. *J. Phys. Rev. E* **57**(3), 2992 (1998)
28. S. Lepri, R. Livi, A. Politi, Thermal conduction in classical low-dimensional lattices. *Phys. Rep.* **377**(1), 1–80 (2003)
29. P. De Gregorio, L. Rondoni, M. Bonaldi, L. Conti, One-dimensional models and thermomechanical properties of solids. *Phys. Rev. B* **84**(22), 224103 (2011)
30. J. Jiang, H. Zhao, Modulating thermal conduction by the axial strain. *J. Stat. Mech.* **2016**(9), 093208 (2016)
31. G. Falasco, F. Baldovin, K. Kroy, M. Baiesi, Mesoscopic virial equation for nonequilibrium statistical mechanics. *NJP* **18**(9), 093043 (2016)
32. C. Mejía-Monasterio, A. Politi, L. Rondoni, Antonio, Heat flux in one-dimensional systems. *Phys. Rev. E* **100**(3), 032139 (2019)
33. R.X.V.I. Clausius, On a mechanical theorem applicable to heat. *Lond. Edinb. Dublin Philos. Mag. J. Sci.* **40**(265), 122–7 (1870)
34. S.G. Das, A. Dhar, O. Narayan, Heat conduction in the  $\alpha$ -  $\beta$  Fermi-Pasta-Ulam chain. *J. Stat. Phys.* **154**, 204–213 (2014)
35. A. Miron, J. Cividini, A. Kundu, D. Mukamel, Derivation of fluctuating hydrodynamics and crossover from diffusive to anomalous transport in a hard-particle gas. *Phys. Rev. E* **99**(1), 012124 (2019)
36. Z. Rieder, J. Lebowitz, E. Lieb, Properties of a harmonic crystal in a stationary nonequilibrium state. *J. Math. Phys.* **8**(5), 1073–1078 (1967)
37. J. Vollmer, L. Rondoni, M. Tayyab, C. Giberti, C. Mejía-Monasterio, Displacement autocorrelation functions for strong anomalous diffusion: a scaling form, universal behavior, and corrections to scaling. *Phys. Rev. Res.* **3**(1), 013067 (2021)